Cardiovascular Engineering and Technology
https://doi.org/10.1007/s13239-024-00733-2

BMES BIOMEDICAL ENGINEERING SOCIETY

ORIGINAL ARTICLE

"What makes blood clots break off?" A Back-of-the-Envelope Computation Toward Explaining Clot Embolization

Osman Gültekin[1] · Matthew J. Lohr[2] · Grace N. Bechtel[2] · Manuel K. Rausch[1,2,3]

Received: 12 December 2023 / Accepted: 3 May 2024

Abstract

Purpose One in four deaths worldwide is due to thromboembolic disease; that is, one in four people die from blood clots first forming and then breaking off or embolizing. Once broken off, clots travel downstream, where they occlude vital blood vessels such as those of the brain, heart, or lungs, leading to strokes, heart attacks, or pulmonary embolisms, respectively. Despite clots' obvious importance, much remains to be understood about clotting and clot embolization. In our work, we take a first step toward untangling the mystery behind clot embolization and try to answer the simple question: "What makes blood clots break off?"

Methods To this end, we conducted experimentally-informed, back-of-the-envelope computations combining fracture mechanics and phase-field modeling. We also focused on deep venous clots as our model problem.

Results Here, we show that of the three general forces that act on venous blood clots—shear stress, blood pressure, and wall stretch-induced interfacial forces—the latter may be a critical embolization force in occlusive and non-occlusive clots, while blood pressure appears to play a determinant role only for occlusive clots. Contrary to intuition and prior reports, shear stress, even when severely elevated, appears unlikely to cause embolization.

Conclusion This first approach to understanding the source of blood clot bulk fracture may be a critical starting point for understanding blood clot embolization. We hope to inspire future work that will build on ours and overcome the limitations of these back-of-the-envelope computations.

Keywords Thromboembolism · Pulmonary hypertension · Embolization · Fracture · Phase-field modeling

Introduction

Blood clots' physiological function is to arrest bleeding upon vascular injury. However, clots can also form pathologically within our vessels. Once formed, clots may break off—or embolize—and travel downstream, where they occlude smaller vessels, such as those of our brain, heart, or lungs. Thereby, clots give rise to a number of deadly diseases including strokes, heart attacks, and pulmonary embolisms [1, 2]. In fact, one in four deaths worldwide is due to thromboembolic diseases, i.e., the formation and breaking off of blood clots [3]. There is a significant body of research on why blood clots form in the first place. In contrast, little is understood about clot embolization [4]. That is, there is no confident answer to the simple question: "What makes blood clots break off?" Given the clinical significance of thromboembolic diseases, finding an answer to this question is not only of scientific interest but also of the utmost medical importance.

During formation, activated platelets and the blood-borne monomer fibrinogen interact in a complex biochemical process to yield the biocomposite blood clot. The fibrinogen monomers polymerize into a 3D biopolymer network called fibrin that forms the structural backbone of clots [5, 6], akin to collagen in connective tissues [7–9]. At the same time, platelets attach to fibrin and, through

Associate Editor Alison Marsden oversaw review of this article.

✉ Manuel K. Rausch
manuel.rausch@utexas.edu

[1] Department of Aerospace Engineering and Engineering Mechanics, The University of Texas at Austin, Austin, TX 78712, USA

[2] Department of Biomedical Engineering, The University of Texas at Austin, Austin, TX 78712, USA

[3] Oden Institute for Computational Engineering and Sciences, The University of Texas at Austin, Austin, TX 78712, USA

their active contractile apparatus, compact the clot and compress entangled red blood cells and other blood components [10, 11].

The exact clot composition, and therefore biophysical properties, vary depending on the location and conditions of clot formation [12]. For example, clots that form on the arterial side do so under relatively high blood pressure (≈ 100 mmHg) and high fluid shear stress (≈ 240 Pa) [13, 14]. In contrast, clots that form on the venous side do so under low blood pressure (≈ 20 mmHg) and low fluid shear stress (≈ 87 Pa) [14–16]. Arterial conditions lead to clots whose structure aligns with the flow direction and are rich in platelets [17]. Venous conditions lead to clots which have random structure and are rich in fibrin [18]. Differing coagulation conditions and, thus, biophysical properties likely lead to quantitatively different answers to our question of interest. Therefore, in our work, we focus on venous clot and its associated diseases, deep vein thrombosis and pulmonary embolism [19]. That is, we will focus on clot that forms in the deep veins of our arms and legs and, when embolizing, may travel downstream to occlude our pulmonary arteries. As this condition affects 300,000–600,000 Americans every year and is one of the leading causes of death during pregnancy and postpartum, it is of high clinical importance in its own right [20, 21].

Given the high prevalence of thromboembolic disease in general and of deep vein thrombosis and pulmonary embolism specifically, our goal is to answer the simple question we posed above: "What makes blood clots break off?" Fundamentally, we know that blood clot breaks off for the same reason that any material breaks or fractures; because the strain energy due to external and internal forces locally exceeds a material-specific fracture threshold called fracture toughness [22]. This fundamental fracture mechanics understanding applies to traditional engineering materials such as steel and aluminum and also to soft materials such as hydrogels, soft tissues, and blood clots. However, exactly which forces impart enough strain energy to exceed clots' fracture toughness is unclear.

Potential candidates for such forces are blood pressure, blood flow-induced shear stress, and interfacial forces between the clot and vessel wall due to wall stretch. While pressure and shear stress are obvious candidates, interfacial force may be a surprising candidate. To understand why we included this force among our candidates, we must recall that veins are 30 times more compliant than arteries [23]. That is, while arteries are primarily conduits for blood flow, the function of veins is that of a blood reservoir. Therefore, veins can expand significantly in both circumference and length. In fact, when removed from the body, veins shrink to 60% of their initial length [24, 25], giving insight into veins' large in vivo stretch. Because of the stiffness mismatch between clot and vessel wall, the in vivo stretch induces large interfacial forces, which to date have remained unexplored as potential drivers for clot embolization.

To give an answer to the question at hand, in vivo methods are not suitable. First, measuring any of our candidate forces is difficult in vivo. That is, fluid shear stress cannot be directly measured but only indirectly inferred. Additionally, shear stress and pressure cannot be decoupled in vivo. Instead, only their coupled effect can be studied. Also, interfacial forces per se cannot be measured in vivo. Similarly, in vitro methods are unsuitable to answer this question because in vitro blood pressure and shear stress also cannot be decoupled. Furthermore, recreating realistic flow conditions and clot geometries is difficult in vitro. Therefore, we chose a computational approach [26]. Specifically, we chose to build idealized 3D representations of occlusive and non-occlusive venous clots and use a non-standard finite element method that involves the phase-field fracture modeling approach to capture the physics of embolization. This approach circumvents the numerical complications arising from the inherently discontinuous (fracture) phenomenon by diffusing the sharp crack surface while capturing complex crack topologies [27, 28]. Note, here we focus on bulk fracture. That is, we do not specifically model the clot–wall interface as a first step towards understanding blood clot embolization.

Methods

In Vitro Blood Clot Experiments

We generated blood clot from whole bovine blood obtained from a commercial service (Lampire Biological Laboratories, PA, USA) where blood is collected directly into CPDA-1 anticoagulant. We added calcium chloride ($CaCl_2$) to a final concentration of 20 mM to reverse the anticoagulant and followed prior protocols to cast the sample into 3D-printed molds compatible with our mechanical testing machine [29]. Our protocol yielded a sample with dimensions of 40 mm by 10 mm by 3 mm, with a total sample volume of 1200 mm^3. We covered the molds to avoid dehydration and incubated the sample at $37°C$ for 60 min. Following incubation, we mounted the sample to our tensile testing machine (Instron, MA, USA). In preparation for mode-I fracture testing, we gave the sample a 13 mm cut on its lateral side. Note, we chose this length to avoid boundary effects impacting our fracture toughness measurements. We then conducted an extension-to-failure experiment at a rate of 0.1 mm/s, corresponding to a strain rate of 1%/s. During the test, we collected force data, displacement data, and images of the fracture process.

Phase-Field Modeling

We model embolization, i.e., clot fracture, within the nonlinear finite element framework using the phase-field approach. Therein, fracture emerges as a coupled problem that we solve for the clots' deformation field and a variable that captures the local damage in response to external forces exceeding the clots' fracture toughness. We capture clots' deformation via the deformation map $\boldsymbol{\varphi}_t$ and the clots' damage via the crack phase-field d. While the deformation map transforms a point $\boldsymbol{X} \in \mathcal{B}$ in the reference state onto its spatial counterpart $\boldsymbol{x} \in \mathcal{S}$, the phase-field continuously interpolates between the intact ($d = 0$) and the fully damaged state of the solid ($d = 1$). For details of the kinematics of the problem, we refer readers to [30–32].

The coupled problem may then be expressed as a rate-type potential Π based on the balance of power, viz.

$$\Pi = \mathcal{E} + \mathcal{D} - \mathcal{P}, \tag{1}$$

where $\mathcal{E}$ denotes the rate of the elastic energy storage and $\mathcal{D}$ accounts for the rate of the energy dissipated due to fracture. Here, $\mathcal{P}$ is the externally supplied power due to the body forces and tractions. As a next step, we consider the variation of the potential in Eq. 1.

The corresponding minimization of the primary field variables yields the governing equations of the mechanical problem, namely the balance of the linear momentum,

$$\mathrm{div}(\boldsymbol{\sigma}) + \boldsymbol{\gamma} = \boldsymbol{0}, \tag{2}$$

as well as the evolution equation of the fracture phase-field,

$$2l(1-d)\mathcal{H} = (d - l^2\Delta d). \tag{3}$$

In Eq. 2, $\boldsymbol{\sigma}$ and $\boldsymbol{\gamma}$ represent the Cauchy stress tensor and the body force vector per unit volume. Equation 3 involves the length-scale parameter l, the damage parameter d, and the driving source term $\mathcal{H}$ that reads

$$\mathcal{H} = \max_{s\in[0,t]} \left\langle \frac{\Psi_0(s)}{g_c} - 1 \right\rangle. \tag{4}$$

Importantly, Eq. 4 ensures irreversibility of fracture—it stores the maximum value in the entire deformation history $[0, t]$—and forms an isotropic criterion for the onset of fracture. Fracture onset only occurs when $\Psi_0(s) \to g_c$. Therein, g_c represents the fracture toughness or the critical energy release rate, while Ψ_0 denotes the deviatoric free energy function of the principal stretch $(\lambda_1, \lambda_2, \lambda_3)$ based on a one-term Ogden model, i.e.,

$$\Psi_0 := \hat{\Psi}_0(\lambda_1, \lambda_2, \lambda_3) = \frac{2\mu}{\alpha^2}(\lambda_1^\alpha + \lambda_2^\alpha + \lambda_3^\alpha - 3), \tag{5}$$

where μ and α describe the shear modulus and the parameter controlling the degree of nonlinearity, respectively, see [33, 34] for more details. Note that the total free energy is the sum of the deviatoric portion, Ψ_0 and a volumetric portion, U, viz.

$$W = \Psi_0 + U. \tag{6}$$

The latter follows from

$$U := \hat{U}(J) = \frac{\kappa(J-1)^2}{2}, \tag{7}$$

with J being the Jacobian of the deformation—i.e., the ratio between the volume in the deformed and the reference configuration—and κ being the bulk modulus. In other words, the bulk modulus serves as a penalty parameter for volume change. Because we only degrade the deviatoric portion of the strain energy, the total energy of a damaged material, thus, reads

$$W = G(d)\Psi_0 + U, \tag{8}$$

where $G(d) = (1-d)^2$. We identified both Ogden parameters using an inverse finite element approach, in which we matched the force–displacement data of our mode-I fracture experiments at strains well below the critical stretch at which fracture occurred. Thereby, we found $\mu = 1.04$ (kPa) and $\alpha = 7.21$. Please note that, in the absence of volumetric experimental data, we chose a bulk modulus of $\kappa = 100$ (kPa) for our simulations, unless indicated otherwise.

In view of the above-stated descriptions, Eqs. 2–3 are discretized in time and space via a Galerkin-type weak formulation and solved for the respective primary field variables, i.e., displacement and phase-field, in the finite element framework. Note, to overcome ill-conditioning of the stiffness matrix in the face of large bulk moduli relative to shear moduli, we implemented a mixed finite element formulation (Q1P0 element). Details of the weak formulation and the algorithmic treatment can be found in [35–37]. Please note that we used the open-source nonlinear finite element solver FEAP to solve the above problem.

Results

Identification of Clot Fracture Toughness from Mode-I Fracture Experiments

Our overall strategy was to use the finite element method and phase-field modeling to compute if and where our candidate external forces exceed the fracture toughness of blood clots. These simulations required information about wall and clot geometry, as well as wall and clot elastic and fracture properties. While we borrowed geometric and wall

properties from the literature, we set out to identify realistic values for clots' elastic and fracture properties from our own experiments. To this end, we coagulated venous blood into a standard pure shear specimen to determine clots' hyperelastic Ogden material parameters as described previously [34]. Additionally, we coagulated venous blood clots into mode-I geometries and conducted fracture tests [38]. Information on sample preparations, coagulation conditions, and other experimental details can be found in the Methods section, and our previous work [29]. Next, we modeled the same mode-I fracture experiment using our phase-field modeling approach. We captured the elastic behavior using a one-term Ogden model, whose elastic parameters were identified using an inverse finite element approach. Figure 1A depicts the corresponding mode-I sample geometry and the finite element discretization with 11,650 elements. We then manually optimized the fracture toughness of our model until our numerically-predicted mode-I force–displacement curves matched the results of our experiments, thus, inversely identifying the fracture toughness g_c of venous blood clots. Figure 1B shows the final match between our experimentally- and numerically-predicted force–displacement curves, yielding a fracture toughness of $g_c = 0.96$ N/m. Furthermore, Fig. 1C shows snapshots of the mode-I fracture simulations, which reveal the evolution of the fracture process: (i) the incipient crack, (ii) the crack growth at the peak force, (iii) the state of crack on the unloading regime, and (iv) the ultimate fracture. The color coding of this figure depicts the (local) damage of the material where a value of $d = 1$ indicates that the material has failed (fractured), while $d = 0$ indicates that the material remains undamaged. Thus, the figure reveals the high damage localization around the fracture site. These images also qualitatively agree with our experimental observations, see Supplementary Fig. S1. Figure 1C also illustrates the corresponding evolution of the Cauchy stress component σ_y at the same four time points. These images highlight the high stress concentrations at the crack tip that indicate the high local energy densities that ultimately drove the fracture propagation.

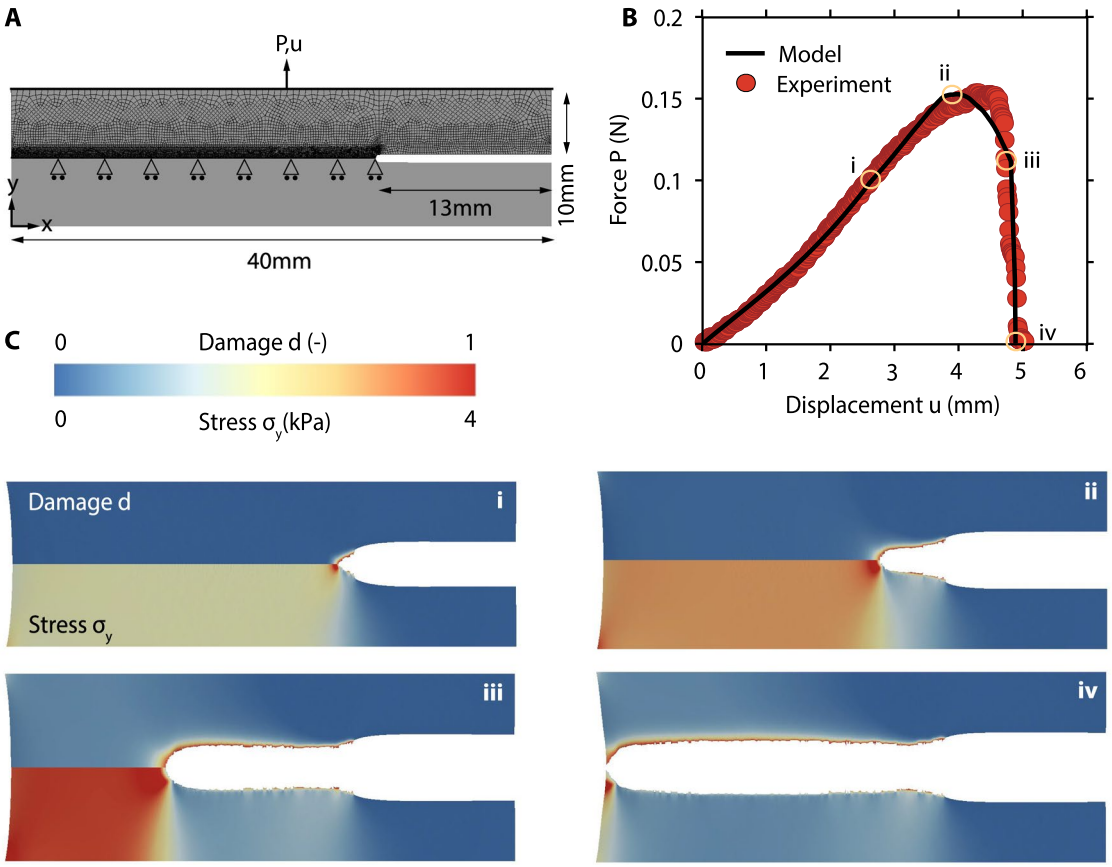

Fig. 1 Phase-field model of clot mode-I fracture agrees well with experimental data. **A** Due to symmetry with respect to the x-axis, only the upper half of the entire clot domain was modeled. **B** Corresponding force–displacement curves obtained from phase-field fracture simulation (black solid line) and mode-I fracture experiments (red circles). **C** The predicted evolution of the damage field (top half) and the Cauchy stress σ_y (bottom half) during mode-I fracture. Time points (i) through (iv) correspond to points along the force–displacement graph in panel B. Finite elements are blanked when $d \geq 0.9$

Simulated Embolization of Occlusive Deep Vein Clots

In the next step, we built two representative thrombotic scenarios: an occlusive venous clot and a non-occlusive venous clot, see Fig. 2A, B. The figure also shows the spatial discretizations of both geometries. The venous wall geometry is that of a popliteal vein, which is one of the most frequent sites of clot formation and embolization, see Fig. 2C [39, 40]. The clot itself was assigned material parameters as identified above, while the venous wall was modeled as isotropic as described in our prior work [41]. Focusing first on the occlusive scenario, we simulated the impact of blood pressures ranging from 10 to 100 mmHg [15, 16] and wall stretches ranging from $\lambda = 1.5$ to 2 [24, 25]. Also, in recognition that blood clot fracture toughness may vary based on patient-specific factors, coagulation conditions, and age, we repeated simulations for multiples and fractions of our experimentally-determined fracture toughness, i.e., $0.1g_c$, $0.25g_c$, $0.5g_c$, g_c, $10g_c$ [42–44]. Here, and in all subsequent simulations, we simulated only one loading and unloading cycle after initial experiments showed little changes during subsequent cycles. See Supplementary Fig. S2 for an exact depiction of the applied boundary conditions. We first observed that wall-stretches of 1.8, 1.9 and 2 led to observable damage zones with increasing significance across our chosen toughness ranges, see Fig. 3A. In fact, the visibility and severity of the damage zone increased proportional to the stretch ratio applied and culminated at $\lambda = 2$, see also Supplementary Fig. S3 for a visualization on a non-occlusive clot. For smaller wall stretches (< 1.8) interfacial forces between wall and clot did not lead to clear damage, see Supplementary Fig. S4A for the results at a stretch of 1.5. Note that—for comparability between the stretched and unstretched cases—here, and in all subsequent figures, we show the results in the Lagrangian configuration, i.e., projected onto the reference configuration. We also found that pressures of 50 mmHg sufficed to lead to observable damage and indication of delamination between clot and wall at fractions of fracture toughness, see Fig. 3B. At higher, superphysiological pressures (i.e., 100 mmHg), pressure also lead to damage and delamination sites at full fracture toughness, see Supplementary Fig. S4B. Interestingly, pressure-induced damage zones did not fully propagate along the clot or diverge into the clot at either pressure. It may thus be speculated that no parts of the clot would break off or embolize under the influence of blood pressure alone. On the other hand, wall stretch of 2 at 25% and 10% toughness lead to damage zones that grew along the clot/wall interface before diverging into the clot, where pieces of the clot could consequently embolize. Please see Supplementary Movie S1 for animations of our simulation results. Also, see Supplementary Fig. S5 for a sensitivity study of above findings to vessel size through which we show that smaller veins lead to an increased importance of wall stretch-induced interfacial forces over blood pressure. That is, because the force due to blood pressure scales quadratically with length, its importance lessens for smaller vessels and increases for larger vessels.

Simulated Embolization of Non-occlusive Deep Vein Clots

We repeated the same simulations for the non-occlusive geometry as shown in Fig. 2B. In addition to exploring the impact of pressure and wall stretch on clot embolization, here we also added the impact of wall shear stress. We explored values ranging from 150 to 800 Pa representing physiological and super-physiological values [14, 44–46]. Note that these pressures were applied to the luminal surface of the clot, while the wall away from the clot was exposed to half the wall stress [46]. Unlike the other two forces, the fluid shear stress is not symmetric with respect to the z-plane. Therefore, instead of one-eight we modeled one-fourth of

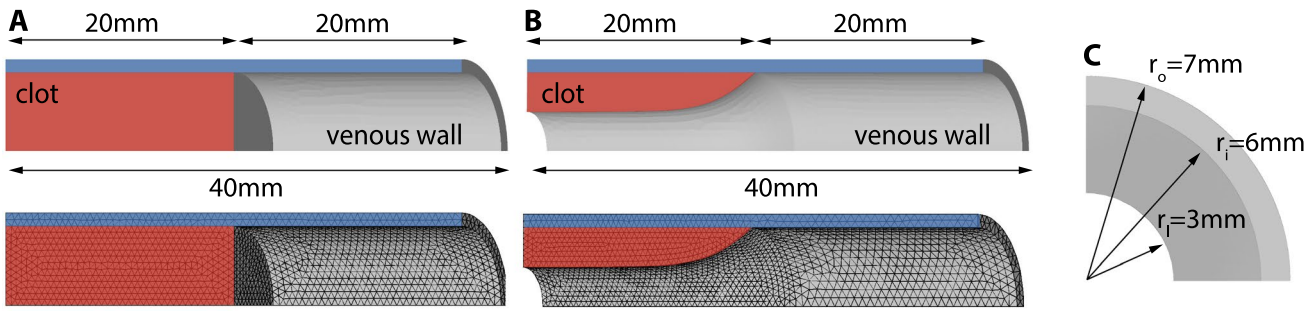

Fig. 2 Model geometries. One-eighth of the clot (red)/vein wall (blue) model for **A,** the fully occlusive case, and **B**, the non-occlusive case and their corresponding mixed tetrahedral finite meshes generated with 60,490 and 65,486 elements, respectively. **C** Cross-sectional view of the clot, the venous wall, and the luminal opening together with their respective radii ($r_i = 3$ mm only for the non-occlusive case). All dimensions shown are in accordance with human popliteal and femoral veins [39, 40]

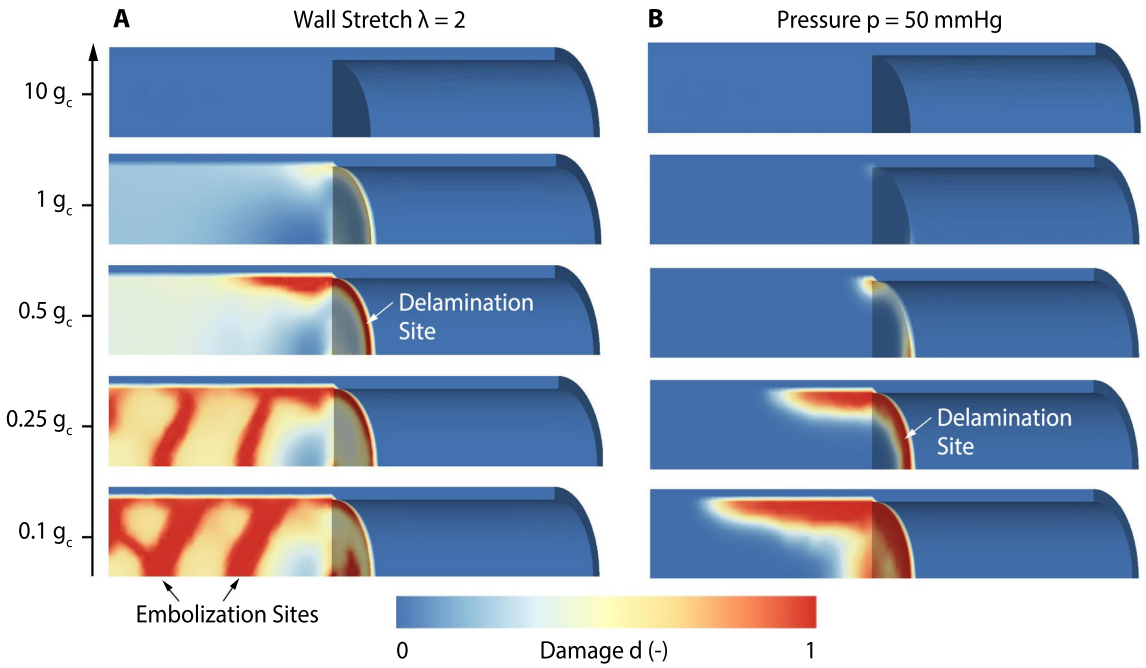

Fig. 3 Occlusive clot: finite element simulations showing the evolution of the damage variable d for multiples and fractions of experimentally determined fracture toughness g_c; **A** axial wall stretch up to $\lambda = 2$ and **B** hydrostatic blood pressure up to $p = 50$ mmHg. Note that $d = 1$ represents the fully damaged state, whereas $d = 0$ indicates the intact state

the entire domain as depicted in the Supplementary Fig. S2. Our findings for the impact of wall stretch-induced damage did not fundamentally differ from our simulation of occlusive clot, see Fig. 4A and Supplementary Fig. S3. That is, at a stretch of $\lambda = 2$ clear signs of damage and delamination are visible for 50% of our originally estimated fracture

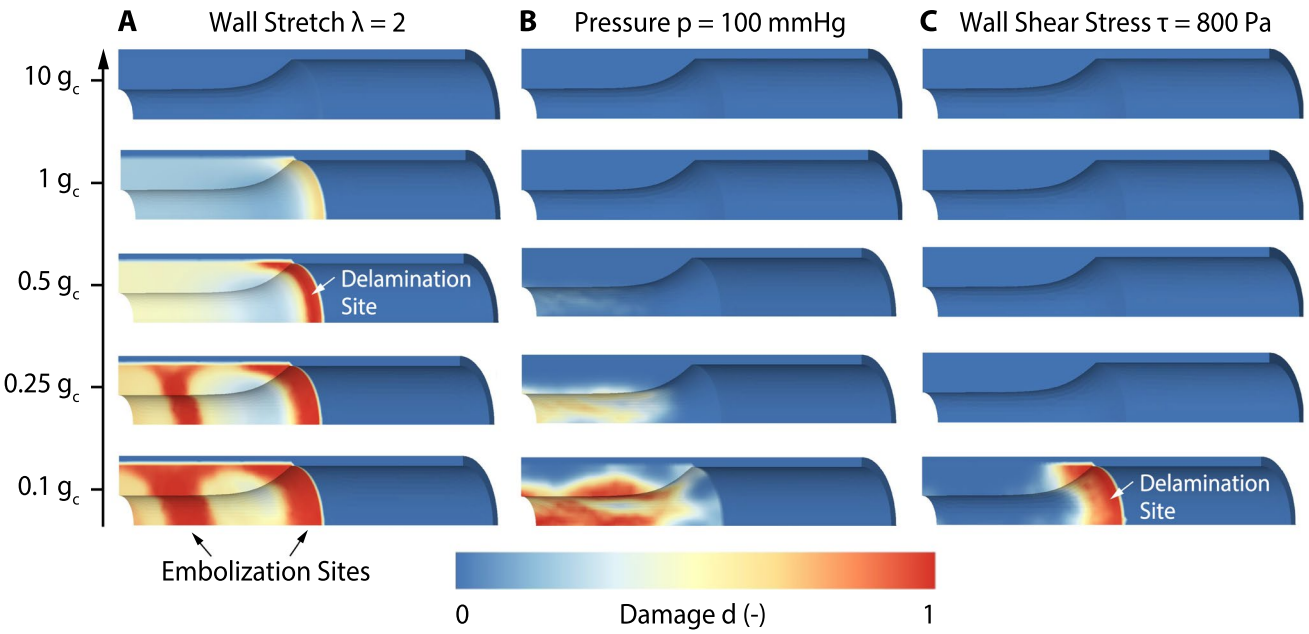

Fig. 4 Non-occlusive clot: finite element simulations showing the evolution of the damage variable d for multiples and fractions of experimentally determined fracture toughness g_c; **A** axial wall stretch up to $\lambda = 2$ and **B** hydrostatic blood pressure up to $p = 100$ mmHg, and **C** wall shear stress up to $\tau = 800$ Pa (here, only half of the computational domain is shown because of space constraints). Note that $d = 1$ represents the fully damaged state, whereas $d = 0$ indicates the intact state

toughness. Interestingly, our findings for pressure did fundamentally differ from our observations in the occlusive geometry, see Fig. 4B. Specifically, for the non-occlusive case blood pressure was barely sufficient to lead to significant damage even at pressures as high as 100 mmHg. In addition to our findings on pressure and wall stretch, we also found that fluid shear stress did not impart significant deformation onto the non-occlusive clot and, therefore, also lead to no or little damage, see Fig. 4C. That is, a super-physiological shear stress of 800 Pa was required to lead to minimal damage and only for 10% fracture toughness. See Supplementary Movie S2 for animations of our simulation results.

Discussion

Clot formation and embolization are the sources of many devastating diseases, including strokes, heart attacks, and pulmonary embolisms. While more is known about why clots form, little is understood about how and why clots embolize. That is, we do not know which forces lead to clot fracture. In our work, we tried to answer this fundamental question using venous blood clots as our model system. To this end, we used two computational models: one of an occlusive blood clot and one of a non-occlusive blood clot. We then combined the finite element modeling framework with the phase-field fracture modeling approach to investigate whether blood pressure, wall–clot-interfacial forces, or fluid shear stress may lead to clot embolization.

Our main finding was that wall shear stress—even when super-physiological—is unlikely to lead to clot fracture and embolization. This came as a surprise to us as wall shear stress is the obvious potential culprit. Instead, we found that only interfacial forces caused by wall stretch lead to significant damage and embolization regardless of clot geometry and vessel size. Blood pressure, on the other hand, drives damage and delamination only in occlusive clots (in large vessels) and, in non-occlusive clot, leads only to minor damage zones even when vastly exaggerated (i.e., as high as 100 mmHg). To the best of our knowledge, this is the first time this observation has been made, which is of both scientific and clinical significance. From a scientific perspective, our findings may inform future experimental and computational studies on clot embolization. Most obviously, future physical and virtual models of clot embolization should include flexible vein walls to accurately reproduce interfacial forces between vein and clot, which they historically have not. Also, future studies of clot embolization should target the clot/wall interface and wall stretch to develop novel therapeutic solutions. From a clinical perspective, our findings may inform therapeutic decision making. For example, clots identified in regions of high vein mobility, such as the knees, may be viewed as higher risk for embolization than others. Thus, more aggressive anti-thrombotic strategies may be chosen. Additionally, our findings suggest that activities that lead to wall stretch should be considered to potentially promote embolization.

It should be noted that damage, and thus potential embolization, occurred in our model only at reduced fracture toughness. This finding may have three potential explanations. First, it may be that our model and its inherent limitations may not perfectly capture the in vivo fracture process. For example, we model both clot and vein wall as perfectly elastic and do not capture potential fatigue behavior, while the in vivo fracture process may occur "sub-critically" under fatigue; that is, at a load that only leads to damage, fragmentation, and embolization after many repetitions. Alternatively, it may be that our in vitro estimate of fracture toughness is an imperfect measure of clots' in vivo fracture toughness. For example, our unnatural in vitro coagulation path may yield non-physiological fracture toughness. Albeit, others have found similar values for fracture toughness of clot from venous blood, thus instilling confidence in our measure [42–44, 47]. Finally, there may be significant inter-subject and inter-species variability in clots' fracture toughness which we have not accounted for due to comorbidities, genetic factors, behavioral factors, and physiological state, such as pregnancy. Importantly, these limitations would affect our findings quantitatively, but not qualitatively. That is, even if true, our key takeaway—that wall stretch-induced interfacial forces and pressure outweigh wall shear stress in their ability to cause embolization—would still hold.

Interestingly, our findings disagree somewhat with the limited prior work on this subject. That is, two prior studies have reported fluid shear stress as a potential cause for clot embolization. For example, Basmadjian et al. [48] estimated the critical wall shear stress leading to embolization to fall between 2.5 and 50 Pa. Recall that we found shear stress as high as 800 Pa to cause little damage in either of our clot models. Discrepancies in our findings likely stem from Basmadjian et al. basing their estimates of embolization risk on single-cell-based measurements of attachment forces. That is, they ignore that the compositional and microstructural complexity of clot likely leads to bulk behavior different from single-cell behavior. Additionally, their work ignores the mechanical complexity of the embolization process, i.e., they ignored clot mechanics (including its fracture) altogether and base their estimation on fluid-mechanical quantities only. Together, these factors likely explain discrepancies between their study and ours. Brass and Diamond [49] also reported clot embolization due to shear stress at values of 240 Pa based on [14]. Their findings are based on microfluidic measurements in combination with fluid simulations. The specific causes for their clots' lower resistance to shear than ours are difficult to identify. However, we assume that different geometries, smaller scales,

and different coagulation conditions may be the sources. Importantly, our work's value lies primarily in the direct comparison between three likely potential culprits and their relative importance. Thus, quantitative discrepancies with the above works have a limited impact on the validity and importance of our work. Nonetheless, it cannot be entirely denied that discrepancies may stem from some of our simplifying modeling assumptions, see more details below. Future studies will hopefully shed additional light on this subject.

Finally, it is important to recall that this is only a first step towards modeling and understanding a very complex phenomenon. Consequently, our work suffers from a number of limitations that we hope future work will overcome. In addition to the limitation mentioned above, here we have not specifically modeled the clot–wall interface. Thus, we implicitly assume that the interfacial toughness is the same as the bulk toughness. Future iterations of this or other models could specifically target and explore interfacial failure using a cohesive element approach [50]. However, we do not expect that accounting for the interfacial toughness would change our qualitative findings. That is, the relative importance between our fundamental failure mechanisms would likely remain the same. Also, note in our current model, shear stress and/or pressure-induced changes to wall and clot deformation do not alter the implied fluid-mechanics of the problem. Namely, we do not account for the impact that wall and clot deformation have on blood flow, which would affect the fluid shear stress and blood pressure. Accounting for these interactions would require a complex fluid–structure-interaction model. We hope that we or others will—in the future—combine phase-field fracture models with fluid–structure-interaction models to increase the accuracy and, thus, confidence in embolization studies. Similarly, time-dependent material effects could, in the future, be included to accurately account for clots poroelastic and viscoelastic properties that could play a critical role in embolization [51, 52]. Additional limitations of our work pertain to the mode of vein wall deformation. We tested vein wall stretch up to 100% strain, albeit rationalized by indirect observations on vein deformability, there is currently no clinical evidence that veins stretch this much in vivo. Hopefully, future in vivo studies will fill this knowledge gap. We have also not explored all possible deformation modes. For example, veins could also be bent and sheared, neither of which we explicitly accounted for. It is also important to note that our in vitro clots were made of venous blood and, thus, have the same composition as fresh intra-venous clot. However, because our in vitro clots were formed under stagnant conditions, rather than under in vivo flow, their microstructure likely differs from "real clots". Finally, the mechanical properties of clots made from cow blood and human blood differ, introducing an additional limitation [53]. Thus, we caution the reader to interpret our findings with these limitation in mind. We look forward to our work being a first step toward future efforts that expand our approach and include additional anatomical and physiological complexities of this process.

Conclusion

In conclusion, we have successfully provided a first answer to the fundamental question: "What makes blood clots break off?" Of our three potential culprits, we have identified interfacial forces due to wall stretch and blood pressure to be the most likely causes. It should be noted, however, that this finding depends on both clot geometry and vessel geometry. Our work begins to fill a gap in our fundamental understanding of the pathophysiology of thromboembolism. Thereby, it—and the work that will build on this current effort—may inform clinical decisions and aid clinicians in treating people that suffer from thromboembolic diseases. Future work will hopefully confirm our findings and expand our work to the arterial side.

Supplementary Information The online version of this article (https://doi.org/10.1007/s13239-024-00733-2) contains supplementary material, which is available to authorized users.

Acknowledgements We acknowledge the financial support from the Office of Naval Research via Grant N00014-22-1-2073 and from the National Science Foundation via Grants 2046148, 2105175, and 2127925.

Data Availability The mechanical test data are available in the Texas Data Repository under https://dataverse.tdl.org/dataverse/STBML.

Declarations

Conflict of interest Manuel K. Rausch has a speaking agreement with Edwards Lifesciences. No other authors have competing interests to report.

References

1. Malone, F., E. McCarthy, P. Delassus, P. Fahy, J. Kennedy, A. Fagan, and L. Morris. The mechanical characterisation of bovine embolus analogues under various loading conditions. *Cardiovasc. Eng. Technol.* 9:489–502, 2018.
2. Fiorella, D. The evolution of stenting and stent-retrieval for the treatment of acute ischemic stroke. *Cardiovasc. Eng. Technol.* 4:352–356, 2013.
3. Wendelboe, A. M., and G. E. Raskob. Global burden of thrombosis: epidemiologic aspects. *Circ. Res.* 118(9):1340–1347, 2016. https://doi.org/10.1161/CIRCRESAHA.115.306841. Accessed 13 Feb 2023.
4. Duval, C., A. Baranauskas, T. Feller, M. Ali, L. T. Cheah, N. Y. Yuldasheva, S. R. Baker, H. R. McPherson, Z. Raslan, M. A. Bailey, et al. Elimination of fibrin γ-chain cross-linking by FXIIIa increases pulmonary embolism arising from

murine inferior vena cava thrombi. *Proc. Natl Acad. Sci. USA*. 118(27):2103226118, 2021.
5. Collet, J.-P., H. Shuman, R. E. Ledger, S. Lee, and J. W. Weisel. The elasticity of an individual fibrin fiber in a clot. *Proc. Natl Acad. Sci. USA*. 102(26):9133–9137, 2005.
6. Kumar, S., Y. Wang, M. Hedayati, F. Fleissner, M. K. Rausch, and S. H. Parekh. Structural control of fibrin bioactivity by mechanical deformation. *Proc. Natl Acad. Sci. USA*. 119(22):2117675119, 2022.
7. Münster, S., L. M. Jawerth, B. A. Leslie, J. I. Weitz, B. Fabry, and D. A. Weitz. Strain history dependence of the nonlinear stress response of fibrin and collagen networks. *Proc. Natl Acad. Sci. USA*. 110(30):12197–12202, 2013.
8. Fleissner, F., M. Bonn, and S. H. Parekh. Microscale spatial heterogeneity of protein structural transitions in fibrin matrices. *Sci. Adv.* 2(7):1501778, 2016. https://doi.org/10.1126/sciadv.1501778. Accessed 27 Feb 2023.
9. Buehler, M. J. Nature designs tough collagen: explaining the nanostructure of collagen fibrils. *Proc. Natl Acad. Sci. USA* 103(33):12285–12290, 2006. https://doi.org/10.1073/pnas.0603216103. Accessed 13 Feb 2023.
10. Kim, O. V., R. I. Litvinov, M. S. Alber, and J. W. Weisel. Quantitative structural mechanobiology of platelet-driven blood clot contraction. *Nat. Commun.* 8(1):1274, 2017.
11. Tutwiler, V., A. R. Mukhitov, A. D. Peshkova, G. Le Minh, R. Khismatullin, J. Vicksman, C. Nagaswami, R. I. Litvinov, and J. W. Weisel. Shape changes of erythrocytes during blood clot contraction and the structure of polyhedrocytes. *Sci. Rep.* 8(1):17907, 2018.
12. Pivkin, I. V., P. D. Richardson, and G. Karniadakis. Blood flow velocity effects and role of activation delay time on growth and form of platelet thrombi. *Proc. Natl Acad. Sci. USA*. 103(46):17164–17169, 2006.
13. Safar, M. E. Arterial stiffness as a risk factor for clinical hypertension. *Nat. Rev. Cardiol.* 15(2):97–105, 2018. https://doi.org/10.1038/nrcardio.2017.155. Accessed 16 May 2023.
14. Colace, T. V., R. W. Muthard, and S. L. Diamond. Thrombus growth and embolism on tissue factor-bearing collagen surfaces under flow: role of thrombin with and without fibrin. *Arterioscler. Thromb. Vasc. Biol.* 32(6):1466–1476, 2012. https://doi.org/10.1161/ATVBAHA.112.249789. Accessed 13 Feb 2023.
15. Eberhardt, R. T., and J. D. Raffetto. Chronic venous insufficiency. *Circulation* 130(4):333–346, 2014. https://doi.org/10.1161/CIRCULATIONAHA.113.006898. Accessed 23 Feb 2023.
16. Tansey, E. A., L. E. A. Montgomery, J. G. Quinn, S. M. Roe, and C. D. Johnson. Understanding basic vein physiology and venous blood pressure through simple physical assessments. *Adv. Physiol. Educ.* 43(3):423–429, 2019. https://doi.org/10.1152/advan.00182.2018. Accessed 13 Feb 2023.
17. Whittaker, P., and K. Przyklenk. Fibrin architecture in clots: a quantitative polarized light microscopy analysis. *Blood Cells Mol. Dis.* 42(1):51–56, 2009.
18. Tan, K. T., and G. Y. Lip. Red vs white thrombi: treating the right clot is crucial. *Arch. Intern. Med.* 163(20):2534–2535, 2003.
19. Mirakhorli, F., B. Vahidi, M. Pazouki, and P. T. Barmi. A fluid–structure interaction analysis of blood clot motion in a branch of pulmonary arteries. *Cardiovasc. Eng. Technol.* 14(1):79–91, 2023.
20. Beckman, M. G., W. C. Hooper, S. E. Critchley, and T. L. Ortel. Venous thromboembolism: a public health concern. *Am. J. Prev. Med.* 38(4):495–501, 2010.
21. James, A. H. Venous thromboembolism in pregnancy. *Arterioscler. Thromb. Vasc. Biol.* 29(3):326–331, 2009.
22. Zhao, X. Designing toughness and strength for soft materials. *Proc. Natl Acad. Sci. USA*. 114(31):8138–8140, 2017.
23. Gelman, S., D. S. Warner, and M. A. Warner. Venous function and central venous pressure: a physiologic story. *J. Am. Soc. Anesthesiol.* 108(4):735–748, 2008.
24. Martinez, R., C. A. Fierro, P. K. Shireman, and H.-C. Han. Mechanical buckling of veins under internal pressure. *Ann. Biomed. Eng.* 38(4):1345–1353, 2010. https://doi.org/10.1007/s10439-010-9929-1. Accessed 16 Feb 2023.
25. Rezakhaniha, R., and N. Stergiopulos. A structural model of the venous wall considering elastin anisotropy. *J. Biomech. Eng.*130(3):031017, 2008. https://doi.org/10.1115/1.2907749. Accessed 16 Feb 2023.
26. Iannaccone, F., M. De Beule, B. Verhegghe, and P. Segers. Computer simulations in stroke prevention: design tools and virtual strategies towards procedure planning. *Cardiovasc. Eng. Technol.* 4:291–308, 2013.
27. Francfort, G. A., and J.-J. Marigo. Revisiting brittle fracture as an energy minimization problem. *J. Mech. Phys. Solids* 46(8):1319–1342, 1998. https://doi.org/10.1016/S0022-5096(98)00034-9. Accessed 6 March 2023.
28. Bourdin, B., G. A. Francfort, and J.-J. Marigo. The variational approach to fracture. *J. Elast.* 91(1–3):5–148, 2008. https://doi.org/10.1007/s10659-007-9107-3. Accessed 6 March 2023.
29. Sugerman, G. P., A. Chokshi, and M. K. Rausch. Preparation and mounting of whole blood clot samples for mechanical testing. *Curr. Protoc.* 1(7), 2021. https://doi.org/10.1002/cpz1.197. Accessed 13 Feb 2023.
30. Miehe, C., F. Welschinger, and M. Hofacker. Thermodynamically consistent phase-field models of fracture: variational principles and multi-field FE implementations. *Int. J. Numer. Methods Eng.* 83(10):1273–1311, 2010. https://doi.org/10.1002/nme.2861. Accessed 6 March 2023.
31. Gültekin, O., H. Dal, and G. A. Holzapfel. A phase-field approach to model fracture of arterial walls: theory and finite element analysis. *Comput. Methods Appl. Mech. Eng.* 312:542–566, 2016. https://doi.org/10.1016/j.cma.2016.04.007. Accessed 6 March 2023.
32. Wu, J.-Y. A unified phase-field theory for the mechanics of damage and quasi-brittle failure. *J. Mech. Phys. Solids* 103:72–99, 2017. https://doi.org/10.1016/j.jmps.2017.03.015. Accessed 6 March 2023.
33. Ogden, R. W. Large deformation isotropic elasticity—on the correlation of theory and experiment for incompressible rubberlike solids. *Proc. R. Soc. Lond. A*. 326(1567):565–584, 1972.
34. Lohr, M. J., G. P. Sugerman, S. Kakaletsis, E. Lejeune, and M. K. Rausch. An introduction to the Ogden model in biomechanics: benefits, implementation tools and limitations. *Philos. Trans. R. Soc. A* 380(2234):20210365, 2022. https://doi.org/10.1098/rsta.2021.0365. Accessed 13 March 2023.
35. Miehe, C., M. Hofacker, and F. Welschinger. A phase field model for rate-independent crack propagation: robust algorithmic implementation based on operator splits. *Comput. Methods Appl. Mech. Eng.* 199(45–48):2765–2778, 2010. https://doi.org/10.1016/j.cma.2010.04.011. Accessed 6 March 2023.
36. Gültekin, O., H. Dal, and G. A. Holzapfel. Numerical aspects of anisotropic failure in soft biological tissues favor energy-based criteria: a rate-dependent anisotropic crack phase-field model. *Comput. Methods Appl. Mech. Eng.* 331:23–52, 2018. https://doi.org/10.1016/j.cma.2017.11.008. Accessed 6 March 2023.
37. Gültekin, O., S. P. Hager, H. Dal, and G. A. Holzapfel. Computational modeling of progressive damage and rupture in fibrous biological tissues: application to aortic dissection. *Biomech. Model. Mechanobiol.* 18(6):1607–1628, 2019. https://doi.org/10.1007/s10237-019-01164-y. Accessed 6 March 2023.
38. Sugerman, G. P., J. Yang, and M. K. Rausch. A speckling technique for DIC on ultra-soft, highly hydrated materials. *Exp.*

Mech. 63(3):585–590, 2023. https://doi.org/10.1007/s11340-023-00938-x. Accessed 17 May 2023.
39. Sadowska, A., J. H. Spodnik, and S. Wójcik. Variations in popliteal fossa venous anatomy: implications for diagnosis of deep-vein thrombosis. *Folia Morphol.* 72(1):51–56, 2013. https://doi.org/10.5603/FM.2013.0008. Accessed 22 May 2023.
40. Keiler, J., R. Seidel, and A. Wree. The femoral vein diameter and its correlation with sex, age and body mass index—an anatomical parameter with clinical relevance. *Phlebol. J. Venous Dis.* 34(1):58–69, 2019. https://doi.org/10.1177/0268355518772746. Accessed 22 May 2023.
41. Rausch, M. K., and J. D. Humphrey. A computational model of the biochemomechanics of an evolving occlusive thrombus. *J. Elast.* 129(1–2):125–144, 2017. https://doi.org/10.1007/s10659-017-9626-5. Accessed 13 Feb 2023.
42. Fereidoonnezhad, B., A. Dwivedi, S. Johnson, R. McCarthy, and P. McGarry. Blood clot fracture properties are dependent on red blood cell and fibrin content. *Acta Biomater.* 127:213–228, 2021. https://doi.org/10.1016/j.actbio.2021.03.052. Accessed 13 Feb 2023.
43. Liu, S., G. Bao, Z. Ma, C. J. Kastrup, and J. Li. Fracture mechanics of blood clots: measurements of toughness and critical length scales. *Extreme Mech. Lett.*.48:101444, 2021. https://doi.org/10.1016/j.eml.2021.101444. Accessed 13 Feb 2023.
44. Garyfallogiannis, K., R. K. Ramanujam, R. I. Litvinov, T. Yu, C. Nagaswami, J. L. Bassani, J. W. Weisel, P. K. Purohit, and V. Tutwiler. Fracture toughness of fibrin gels as a function of protein volume fraction: mechanical origins. *Acta Biomater.* 159:49–62, 2023. https://doi.org/10.1016/j.actbio.2022.12.028. Accessed 15 March 2023.
45. Sakariassen, K. S., L. Orning, and V. T. Turitto. The impact of blood shear rate on arterial thrombus formation. *Future Sci. OA* 1(4):15–28, 2015. https://doi.org/10.4155/fso.15.28. Accessed 13 Feb 2023.
46. Zhao, Y. C., P. Vatankhah, T. Goh, R. Michelis, K. Kyanian, Y. Zhang, Z. Li, and L. A. Ju. Hemodynamic analysis for stenosis microfluidic model of thrombosis with refined computational fluid dynamics simulation. *Sci. Rep.* 11(1):6875, 2021. https://doi.org/10.1038/s41598-021-86310-2. Accessed 13 Feb 2023.
47. Tutwiler, V., J. Singh, R. I. Litvinov, J. L. Bassani, P. K. Purohit, and J. W. Weisel. Rupture of blood clots: mechanics and pathophysiology. *Sci. Adv.* 6(35):0496, 2020. https://doi.org/10.1126/sciadv.abc0496. Accessed 24 March 2023.
48. Basmadjian, D. Embolization: critical thrombus height, shear rates, and pulsatility. Patency of blood vessels. *J. Biomed. Mater. Res.* 23(11), 1315–1326, 1989. https://doi.org/10.1002/jbm.820231108. Accessed 27 Feb 2023.
49. Brass, L. F., and S. L. Diamond. Transport physics and biorheology in the setting of hemostasis and thrombosis. *J. Thromb. Haemostasis* 14(5):906–917, 2016. https://doi.org/10.1111/jth.13280. Accessed 13 Feb 2023.
50. McKenzie, A. J., B. J. Doyle, and Z. M. Aman. Micromechanical force measurement of clotted blood particle cohesion: understanding thromboembolic aggregation mechanisms. *Cardiovasc. Eng. Technol.* 13(6):816–828, 2022.
51. Sugerman, G. P., S. H. Parekh, and M. K. Rausch. Nonlinear, dissipative phenomena in whole blood clot mechanics. *Soft Matter* 16(43):9908–9916, 2020. https://doi.org/10.1039/D0SM01317J. Accessed 13 Feb 2023.
52. Ghezelbash, F., S. Liu, A. Shirazi-Adl, and J. Li. Blood clot behaves as a poro-visco-elastic material. *J. Mech. Behav. Biomed. Mater.* 128:105101, 2022. https://doi.org/10.1016/j.jmbbm.2022.105101. Accessed 13 Feb 2023.
53. Sugerman, G. P., G. N. Bechtel, Z. Malinowska, S. H. Parekh, and M. K. Rausch. Mechanical properties of clot made from human and bovine whole blood differ significantly. *J. Mech. Behav. Biomed. Mater.*154:106508, 2024.